Joint Active and Passive Beamforming in RIS-Assisted Covert Symbiotic Radio Based on Deep Unfolding

Xiuli He, Hongbo Xu, Ji Wang, Wenwu Xie, Xingwang Li, *Senior Member, IEEE*, and Arumugam Nallanathan, *Fellow, IEEE*

***Abstract*—In this paper, we consider an reconfigurable intelligent surface (RIS)-assisted multiple input single output (MISO) covert symbiotic radio (SR) communication system. RIS, as a secondary transmitter (STx), can enhance primary transmission from the primary transmitter (PTx) to the primary receiver (PRx). Simultaneously, STx transmits its own information to the secondary receiver (SRx). In addition, RIS-assisted covert communications have a broad development prospect, and covert communication is considered in which Willie eavesdrops passive signals from RIS (Alice) to SRx (Bob). By jointly optimizing active beamforming vector at PTx and passive beamforming matrix at RIS, the achievable rate of PRx is maximized subject to the covertness constraint and the signal-to-noise ratio (SNR) constraint for secondary transmission. The optimization problem is challenging because of the non-convex objective function and the coupling between variables. Thus, the deep unfolding algorithm based on gradient descent (DUAGD) is proposed for the beamforming design. Specifically, we first transform the optimization problem with constraints into the dual domain. Then inspired by gradient descent algorithm, deep unfolding unfolds the original iterative process into a multi-layer network structure. Results from simulations show that the proposed algorithm has fast convergence while maintaining performance.**

***Index Terms*—Covert communication, deep unfolding, reconfigurable intelligent surface, symbiotic radio.**

I. Introduction

Since a large number of private information needs to be transmitted in both civilian and military fields, the security of information is a key issue, and conventional security methods such as physical layer security technology have been developed to solve this problem [1]. Different from the security of data transmission of conventional methods, covert communication, as a new technology, can ensure that the transmission behavior is not detected [2]. Although adding artificial noise interference and cooperating relays can be used to improve the covertness performance, additional system resources will be consumed. Fortunately, reconfigurable intelligent surface (RIS) can be deployed to provide additional links to improve covert communication performance [3]. As shown in [1], RIS has brought great benefits to covert communication. In addition, symbiotic radio (SR) technology developed based on ambient backscatter communications can solve the challenge of increasing demand for communication resources [4]. However, it may be attacked by malicious eavesdroppers because of its structures. The application of covert communication to the SR system can ensure spectrum efficiency and information covertness [5].

However, the resultant expression of minimum detection error probability contains incomplete gamma functions, which makes the subsequent optimization challenging. To solve this problem, several recent works adopted Kullback-Leibler (KL) divergence to evaluate covertness [2], [6]. In [2], the authors studied the robust transmission design where the KL divergence was adopted in the covert constraint for the IRS-assisted covert communication system. And an alternative optimization (AO) method is proposed to solve this optimization problem. In addition, the authors in [6] adopted Bernstein-type inequality to derive the upper bound of KL divergence to rewrite the covert constraint. The sub-problems of optimization problems are solved by semi-definite programming and penalty successive convex approximation, respectively. The above works are the RIS-assisted active covert communications and these algorithms require complicated mathematical deduction, which is difficult to realize in practice.

Deep learning (DL) inspired by artificial intelligence can solve this problem [7]. The main idea of data-driven DL is to find a mapping from the environmental parameters to the optimal decision by using a deep neural network (DNN), which the DNN can be trained offline by a large number of samples, and the network parameters are fixed in the online testing process to obtain the optimal decision [8]. In the low complexity test process of beamforming optimization, DNNs directly output the optimal beamforming after inputting the channel samples. However, DNN has two main limitations: it is not suitable for solving optimization problems with constraints and has poor interpretability. The model-driven deep unfolding (DU) technique, in contrast to the black-box model approach, allows the construction of a learning network

This work was supported in part by the National Natural Science Foundation of China under Grant 62101205, and in part by the Key Research and Development Program of Hubei Province under Grant 2023BAB061. *(Corresponding author: Ji Wang.)*

Xiuli He, Hongbo Xu, and Ji Wang are with the Department of Electronics and Information Engineering, College of Physical Science and Technology, Central China Normal University, Wuhan 430079, China (e-mail: 2021112301h@mails.ccnu.edu.cn; xuhb@ccnu.edu.cn; jiwang@ccnu.edu.cn).

Wenwu Xie is with the School of Information Science and Engineering, Hunan Institute of Science and Technology, Yueyang 414006, China (e-mail: gavinxie@hnist.edu.cn).

Xingwang Li is with the School of Physics and Electronic Information Engineering, Henan Polytechnic University, Jiaozuo 454003, China (e-mail: lixingwang@hpu.edu.cn).

Arumugam Nallanathan is with the School of Electronic Engineering and Computer Science, Queen Mary University of London, E1 4NS London, U.K. (e-mail: a.nallanathan@qmul.ac.uk).

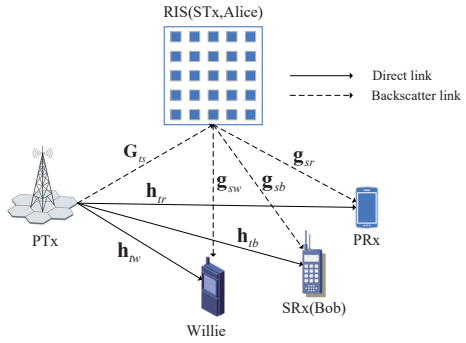

Fig. 1. RIS-assisted downlink MISO covert SR communication system.

that approximating known iterative algorithms using finite iterations, and the iterative steps of optimization algorithms are imitated by the learning networks [9]. For example, in order to solve the computational complexity problem of the weighted minimum mean square error (WMMSE) algorithm, the authors of [10] applied the deep unfolding in WMMSE algorithm. In [11], the authors proposed a DU algorithm based on gradient descent (GD) to solve a design problem of hybrid analog-digital transceiver. These algorithms can reduce the computational complexity while maintaining performance.

In this paper, a passive RIS-assisted MISO covert SR communication system is considered, in which KL divergence is adopted to measure covertness. In this system, the eavesdropper Willie detects the passive signals from RIS (Alice) to SRx (Bob), which is more covert. We aim to maximize the achievable rate of PTx by jointly optimizing the active and passive beamforming under the covertness constraint and the secondary transmission signal-to-noise ratio (SNR) constraint. Due to the variable coupling and non-convex objective function, the optimization problem is challenging. Furthermore, Willie is not a legitimate user, it is difficult for PTx and Alice to get his instantaneous channel state information (CSI). To solve the complex optimization problem, we first take into account a more realistic application scenario that PTx and Alice only know the Willie's statistical CSI and average over a mini-batch of channel samples to approximate the expectation in covertness constraint [12]. Moreover, a DU algorithm based on GD (DUAGD) is proposed to design beamforming. Specifically, the Lagrangian duality method is adopted to transform the optimization problem with constraints into the dual problem. For the design of the network layer, the GD algorithm is unfolded into a multi-layer network structure, in which each layer in the DU neural network consists of four modules for updating active beamforming, passive beamforming, and Lagrange multipliers.

II. System Model

As shown in Fig. 1, we consider an RIS-assisted covert SR communication system consisting of a PTx with L antennas, an RIS with M reflection units, a PRx with a single-antenna and a single-antenna SRx.

A. Channel Model

A flat-fading channel model is considered, in which the coefficients of channel are constant within a block but may change within different blocks. We denote the complex baseband equivalent channels from PTx to PRx, from PTx to Bob, from PTx to RIS, from PTx to Willie, from RIS to PRx, from RIS to Bob, and from RIS to Willie are $\mathbf{h}_{tr} \in \mathbb{C}^{1\times L}$, $\mathbf{h}_{tb} \in \mathbb{C}^{1\times L}$, $\mathbf{G}_{ts} \in \mathbb{C}^{M\times L}$, $\mathbf{h}_{tw} \in \mathbb{C}^{1\times L}$, $\mathbf{g}_{sr} \in \mathbb{C}^{1\times M}$, $\mathbf{g}_{sb} \in \mathbb{C}^{1\times M}$ and $\mathbf{g}_{sw} \in \mathbb{C}^{1\times M}$, respectively. Furthermore, under the assumption that the transmission signal of PTx in the n-th channel use is $s(n) \sim \mathcal{CN}(0,1)$,$\forall n \in \{1,2,\cdots,N\}$. $\mathbf{f} \in \mathbb{C}^{L\times 1}$ is defined as the transmission beamforming vector of PTx, therefore the transmission signal at PTx is expressed as $\mathbf{f}s(n)$. We define $\mathbf{\Phi} = \mathrm{diag}(\phi_1,\phi_2,\cdots,\phi_{\mathrm{M}})$, where $\phi_i = \rho_i e^{j\theta_i}, i = 1,2\cdots M$, as the diagonal reflection matrix of RIS. For the i-th reflection element of RIS, $\rho_i \in [0,1]$ represents the reflection amplitude, and $\theta_i \in (0,2\pi]$ represents the phase shift. For simplicity, we set $\rho_i = 1, i = 1,2\cdots M$, thus $|\phi_i| = 1$. c denotes the transmitted symbol at RIS, and RIS adopts the binary phase shift keying modulation scheme for incident signal from PTx, i.e, $c = \{0,1\}$. When $c = 1$, RIS sends the symbol '1' by reflecting the signals from PTx, otherwise RIS sends the symbol '0' which means that RIS does not reflect the signals. We assume that each symbol period of c contains N symbol periods of $s(n)$ [13]. Then the reflection signal from PTx is written as $\mathbf{\Phi}\mathbf{G}_{ts}\mathbf{f}s(n)c$.

B. Signal Model

1) Received Signal at PRx: The received signal of PRx in a secondary symbol period is written as

$$y_r(n) = \mathbf{h}_{tr}\mathbf{f}s(n) + \mathbf{g}_{sr}\mathbf{\Phi}\mathbf{G}_{ts}\mathbf{f}s(n)c + u_r(n), \tag{1}$$

where $u_r(n) \sim \mathcal{CN}(0,\sigma_r^2)$ represents the complex Gaussian noise at PRx. When decoding $s(n)$, the backscattering link can be considered as a multi-path component since the symbol period of c is significantly larger than the symbol period of $s(n)$ [13]. Therefore, the signal-plus-noise covariance can be expressed as

$$\Gamma_r = \frac{|(\mathbf{h}_{tr} + c\mathbf{g}_{sr}\mathbf{\Phi}\mathbf{G}_{ts})\mathbf{f}|^2}{\sigma_r^2}. \tag{2}$$

It can be seen that Γ_r depends on c, which changes faster than the channel variation. The achievable rate of PTx is established based on the expectation over c [14], which is represented as

$$R_r = \mathbb{E}_c\left[\log_2(1+\Gamma_r)\right]. \tag{3}$$

2) Received Signal at SRx (Bob): In a secondary symbol period, Bob receives the direct link signal from PTx and the backscattering link signal from RIS. As such, the received signal at Bob, $\mathbf{y}_b(n)$ for $n = 1,2,\cdots,N$, can be written as

$$y_b(n) = \mathbf{h}_{tb}\mathbf{f}s(n) + \mathbf{g}_{sb}\mathbf{\Phi}\mathbf{G}_{ts}\mathbf{f}s(n)c + u_b(n), \tag{4}$$

where $u_b(n) \sim \mathcal{CN}(0,\sigma_b^2)$ represents the complex Gaussian noise at Bob. Bob first decodes $s(n)$ and obtains an estimate of the primary signal $\hat{s}(n)$. Then the primary signal component $\mathbf{h}_{tb}\mathbf{f}\hat{s}(n)$ is subtracted from the received signal $y_b(n)$, and the primary signal is assumed to be completely removed. Thus,

the SNR of decoding c is given in detail in Appendix A, which is approximately written as

$$\gamma_b = \frac{N|\mathbf{g}_{sb}\mathbf{\Phi}\mathbf{G}_{ts}\mathbf{f}s\,(n)|^2}{\sigma_b^2}. \tag{5}$$

3) Received Signal at Willie: In a secondary symbol period, Willie receives the signals from PTx and RIS can be given by

$$y_w(n) = \mathbf{h}_{tw}\mathbf{f}s(n) + \mathbf{g}_{sw}\mathbf{\Phi}\mathbf{G}_{tr}\mathbf{f}cs(n) + u_w(n), \tag{6}$$

where $u_w(n) \sim \mathcal{CN}(0, \sigma_w^2)$ represents the complex Gaussian noise at Willie. The following two hypotheses are distinguished by Willie to detect whether Alice is transmitting signals. We study a worst-case covert communication in this paper. Willie, as an eavesdropper, is detecting to the passive information of RIS. However, Willie's received signal of the direct link from PTx is much stronger than its received signal of the reflected link from RIS. This will result in a significant increase in the error probability of Willie's detection. For Willie, we assume that it first adopts interference cancellation to remove the signal $\mathbf{h}_{tw}\mathbf{f}s(n)$ which acts as interference to the received signal [13]. Then the two hypotheses can be represented as

$$\tilde{y}_w(n) = \begin{cases} n_w(n), & \mathcal{H}_0, \\ \mathbf{g}_{sw}\mathbf{\Phi}\mathbf{G}_{ts}\mathbf{f}cs(n) + n_w(n), & \mathcal{H}_1, \end{cases} \tag{7}$$

where $\mathcal{H}_0$ denotes null hypothesis, which means that Alice does not transmit information, while $\mathcal{H}_1$ denotes alternative hypothesis, which means that Alice has messages to send to SRx. Following (7), the false alarm rate is denoted as $\Pr\{\mathcal{R}_1|\mathcal{H}_0\}$ and the miss detection rate is denoted as $\Pr\{\mathcal{R}_0|\mathcal{H}_1\}$, where $\mathcal{R}_0$ and $\mathcal{R}_1$ are the binary decisions of whether Alice transmits information. Then Willie's total detection error probability is given by

$$\xi = \pi_0 \Pr\{\mathcal{R}_1|\mathcal{H}_0\} + \pi_1 \Pr\{\mathcal{R}_0|\mathcal{H}_1\}, \tag{8}$$

where π_0 and π_1 are the prior probability of hypothesis. We assume $\pi_0 = \pi_1 = 1/2$, and this assumption of equal prior probability is widely adopted in the literature of covert communication [3], [15]. According to Neyman-Pearson criterion, the likelihood ratio test is exploited by Willie to detect passive transmission which is the optimal test that minimizes its error probability [3], and it is given by

$$\frac{\mathbb{P}_1 \triangleq \prod_{n=1}^{N} f(\tilde{y}_w(n)|\mathcal{H}_1)}{\mathbb{P}_0 \triangleq \prod_{n=1}^{N} f(\tilde{y}_w(n)|\mathcal{H}_0)} \underset{\mathcal{R}_1}{\overset{\mathcal{R}_0}{\gtrless}} 1, \tag{9}$$

where the likelihood functions of Willie's observation vector under $\mathcal{H}_0$ and $\mathcal{H}_1$ are $\mathbb{P}_0$ and $\mathbb{P}_1$, respectively. The likelihood functions for $\tilde{y}_w[n]$ in $\mathcal{H}_0$ and $\mathcal{H}_1$ are $f(\tilde{y}_w(n)|\mathcal{H}_0) = \mathcal{CN}(0, \sigma_w^2)$ and $f(\tilde{y}_w(n)|\mathcal{H}_1) = \mathcal{CN}(0, R_w + \sigma_w^2)$, respectively, where $R_w = |\mathbf{g}_{sw}\mathbf{\Phi}\mathbf{G}_{ts}\mathbf{f}|^2$. The minimum detection error rate P_e at Willie can be obtained according to (9) [16]. Thus, $P_e > 1-\varepsilon$ can be used as the covertness constraint for a given ε.

C. Problem Formulation

The objective of this paper is to jointly optimize the active and the passive beamforming to maximize the achievable rate of PRx, subject to the constraint of SNR, the covertness constraint, the power constraint at PTx and the unit-modulus constraint of RIS reflection coefficients. Therefore, the problem can be formulated as

$$(\mathrm{P1}): \max_{\mathbf{f},\mathbf{\Phi}} \quad \mathbb{E}_c\left[\log_2(1+\Gamma_r)\right] \tag{10}$$

$$\text{s.t.} \quad \frac{N|\mathbf{g}_{sb}\mathbf{\Phi}\mathbf{G}_{ts}\mathbf{f}s\,(n)|^2}{\sigma_b^2} \geq \gamma_o, \tag{10a}$$

$$P_e > 1-\varepsilon, \tag{10b}$$

$$\|\mathbf{f}\|^2 \leq P_s, \tag{10c}$$

$$|\phi_i| = 1, \forall i = 1, 2, \cdots, M, \tag{10d}$$

where γ_o denotes the SNR required by secondary transmission, and P_s is the maximum transmitting power. In addition, (10a) is the SNR of secondary transmission and (10b) is the covertness constraint. Constraint (10c) represents the maximum transmitted power satisfied by PTx. (10d) is the unit-modulus constraint on phase shift of RIS reflection elements.

Assume RIS sends the symbol '0' and symbol '1' with equal probability. Thus, in (P1), the expectation of objective function over c can be given by

$$R_r = \frac{1}{2}\log_2(1 + \frac{|(\mathbf{h}_{tr} + \mathbf{g}_{sr}\mathbf{\Phi}\mathbf{G}_{ts})\mathbf{f}|^2}{\sigma_r^2}) + \frac{1}{2}\log_2(1 + \frac{|(\mathbf{h}_{tr}\mathbf{f}|^2}{\sigma_r^2}). \tag{11}$$

Since the resultant expression of P_e involves incomplete gamma function, the subsequent design of constraint (10b) is difficult, as such we adopt the lower bound of P_e to solve this issue [3], which is given by

$$P_e \geq 1 - \sqrt{\frac{1}{2}\mathcal{D}(\mathbb{P}_0 \parallel \mathbb{P}_1)}, \tag{12}$$

where $\mathcal{D}(\mathbb{P}_0 \parallel \mathbb{P}_1) = N\left[\ln(\frac{\mathbf{R}_w+\sigma_w^2}{\sigma_w^2}) - \frac{\mathbf{R}_w}{\mathbf{R}_w+\sigma_w^2}\right]$ is the KL divergence from $\mathbb{P}_0$ to $\mathbb{P}_1$.

In the constraint (10b), the level of covertness is determined by a small value ε. As per (12), $\mathcal{D}(\mathbb{P}_0 \parallel \mathbb{P}_1) \leq 2\varepsilon^2$ relative to $P_e \geq 1-\varepsilon$ is a much stringent constraint. As such, the covertness constraint is reformulated as $\mathcal{D}(\mathbb{P}_0 \parallel \mathbb{P}_1) \leq 2\varepsilon^2$ [15]. In addition, Willie is not a legitimate user, Willie's CSI may not always be accessible to PTx and Alice. We consider a more practical application scenario that PTx and Alice only know the statistical CSI of $\mathbf{g}_{sw}$, while its instantaneous realizations are unknown. Therefore, the expectation of $\mathcal{D}(\mathbb{P}_0 \parallel \mathbb{P}_1)$ serves as the measure of covertness, which can be represented as $\mathbb{E}_{\mathbf{g}_{sw}}[\mathcal{D}(\mathbb{P}_0 \parallel \mathbb{P}_1)]$ that has no closed-form expression. In addition, not only the objective function is non-convex, but also there is coupling between variables. As such, it is a challenging task to design an optimization algorithm to solve this problem.

For the complex optimization problem, we transform the problem with constraints into Lagrangian dual domain. Two Lagrange multipliers λ_1 and λ_2 are associated with (10a) and (10b), respectively. The Lagrangian of (10) can be written as

$$\begin{aligned} L = &- R_r + \lambda_1(\gamma_o - \frac{N|(\mathbf{g}_{sb}\mathbf{\Phi}\mathbf{G}_{ts})\,\mathbf{f}|^2}{\sigma_b^2}) \\ &+ \lambda_2(\mathbb{E}_{\mathbf{g}_{sw}}[\mathcal{D}(\mathbb{P}_0 \parallel \mathbb{P}_1)] - 2\varepsilon^2). \end{aligned} \tag{13}$$

Under the definition of Lagrangian, we denote the dual function $D(\lambda_1, \lambda_2)$ as the minimum Lagrangian value for all $\mathbf{f}$ and

$\mathbf{\Phi}$, which can be given by

$$D(\lambda_1,\lambda_2) := \min_{\mathbf{f},\mathbf{\Phi}} \ L \quad \text{s.t.} \quad (10c),(10d). \tag{14}$$

For any choice of $\lambda_1 \geq 0$ and $\lambda_2 \geq 0$, it can be easily verified that $D(\lambda_1,\lambda_2) \leq \mathrm{P1}^*$. In the dual problem, we search the Lagrange multipliers that make $D(\lambda_1,\lambda_2)$ as large as possible

$$D^* := \max_{\lambda_1,\lambda_2\geq 0} D(\lambda_1,\lambda_2) \quad \text{s.t.} \quad (10c),(10d). \tag{15}$$

When (14) is used as a proxy for (10), the best approximation of (P1) is the dual optimal D^*. As such, (P1) is expressed as

$$(\mathrm{P2}): \max_{\lambda_1,\lambda_2\geq 0} \min_{\mathbf{f},\mathbf{\Phi}} \ L \quad \text{s.t.} \quad (10c),(10d). \tag{16}$$

However, (P2) is a NP-hard problem due to the constraint (10d), its solution procedure is still challenging. Owing to the strong performance in function approximation, DNN can be explored to solve (P2).

III. Deep Unfolding Algorithm Based on Lagrangian Duality

In this section, we first realize the joint design of active and passive beamforming by using GD algorithm. On the basis of GD, the DUAGD is proposed to solve (P2) by jointly design the beamforming.

A. Optimization Algorithm Based on GD

To rewrite the $\mathbb{E}_{\mathbf{g}_{sw}}[\mathcal{D}(\mathbb{P}_0 \parallel \mathbb{P}_1)]$ in a deterministic form, the method of sample average approximation (SAA) is adopted [17]. The approach of SAA approximates the expected objective or constraint functions through sample average estimation, where we generate sample data from the underlying distribution [18]. In our algorithm, the sample $\{\hat{\mathbf{g}}_{sw}^1, \hat{\mathbf{g}}_{sw}^2, \cdots, \hat{\mathbf{g}}_{sw}^{N_a}\}$ is given, where N_a is the size of mini-batch. As such, the $\mathbb{E}_{\mathbf{g}_{sw}}[\mathcal{D}(\mathbb{P}_0 \parallel \mathbb{P}_1)]$ is written as

$$\begin{aligned}\mathbb{E}_{\mathbf{g}_{sw}}[\mathcal{D}(\mathbb{P}_0 \parallel \mathbb{P}_1)] &= \mathbb{E}_{\mathbf{g}_{sw}}\big[N\big[\ln(\frac{\mathbf{R}_w+\sigma_w^2}{\sigma_w^2}) - \frac{\mathbf{R}_w}{\mathbf{R}_w+\sigma_w^2}\big]\big] \\ &= \frac{1}{N_a}\sum_{n=1}^{N_a} N\big[\log(1+\frac{\mathbf{R}_w}{\sigma_w^2}) - 1 + \frac{\sigma_w^2}{\mathbf{R}_w+\sigma_w^2}\big].\end{aligned} \tag{17}$$

The GD algorithm is a first-order optimization algorithm widely used in the fields of deep learning. Specifically, the updated equations of optimization variables in the GD algorithm at the t-th iteration can be written as

$$\begin{aligned}\mathbf{f}^{t+1} &= \mathbf{f}^t - \mu_{\mathbf{f}}\nabla_{\mathbf{f}^t} L, \\ \mathbf{\Phi}^{t+1} &= \mathbf{\Phi}^t - \mu_{\mathbf{\Phi}}\nabla_{\mathbf{\Phi}^t} L, \\ \lambda_1^{t+1} &= \lambda_1^t + \mu_{\lambda_1}\nabla_{\lambda_1^t} L, \\ \lambda_2^{t+1} &= \lambda_2^t + \mu_{\lambda_2}\nabla_{\lambda_2^t} L,\end{aligned} \tag{18}$$

where $t \in \{0,1,\ldots\}$ is iteration index and $\{\mu_{\mathbf{f}}, \mu_{\mathbf{\Phi}}, \mu_{\lambda_2}, \mu_{\lambda_2}\}$ are the step sizes selected based on experiments and experience. The $\nabla_{\mathbf{f}} L$, $\nabla_{\mathbf{\Phi}} L$, $\nabla_{\lambda_1} L$ and $\nabla_{\lambda_2} L$ are the gradients of L to variables $\mathbf{f}$, $\mathbf{\Phi}$, λ_1 and λ_2, respectively. Alternately updating the optimization variables until the L satisfies certain convergence criterion. In order to meet the maximum transmitted power limitation (10c), the active beamforming $\mathbf{f}$ of PTx needs to be scaled at the end of each GD iteration, which can be given by

$$\mathbf{f} = \begin{cases} \mathbf{f}, & \text{if } \|\mathbf{f}\|^2 \leq P_s, \\ \frac{\mathbf{f}}{\|\mathbf{f}\|}\sqrt{P_s}, & \text{otherwise.} \end{cases} \tag{19}$$

To implement the unit modulus constraint of RIS (10d), the passive beamforming $\mathbf{\Phi}$ of RIS at the end of each iteration are scaled, which can be expressed as

$$\mathbf{\Phi} = \mathrm{diag}(\mathrm{e}^{j\varphi_1}, \mathrm{e}^{j\varphi_2}, \cdots, \mathrm{e}^{j\varphi_M}), \tag{20}$$

where φ_i is the output of the i-th element of the diagonal matrix, where $i = 1,2,\cdots,M$. Considering the Lagrange multipliers in (P2) are non-negative, the λ_1 and λ_2 are transformed according as follows

$$\lambda \leftarrow [\lambda]^+, \tag{21}$$

where $[\lambda]^+ = \max[0,\lambda]$.

B. Deep Unfolding Algorithm Based on GD

In the following, we describe the DU neural network structure induced by the GD algorithm developed above. The basic idea of DU is to unfold the iteration of the GD algorithm into the trainable layer of the neural network, where the number of iterations is fixed according to the complexity of the algorithm, which is the number of layers [10]. In the k-th layer of i-th iteration of the DU network, $k \in \{1,\ldots,K\}$, we introduce trainable parameters $\{\mu_{\mathbf{f},i}^k, \mu_{\mathbf{\Phi},i}^k, \mu_{\lambda_1,i}^k, \mu_{\lambda_2,i}^k\}$ to replace the step sizes $\{\mu_{\mathbf{f}}, \mu_{\mathbf{\Phi}}, \mu_{\lambda_1}, \mu_{\lambda_2}\}$ of GD algorithm. In addition, for the training parameters, in order to increase their degrees of freedom, we augment the dimensions of these trainable parameters and introduce the offset parameters $\{\mathbf{q}_{\mathbf{f},i}^k, \mathbf{q}_{\mathbf{\Phi},i}^k, \mathbf{q}_{\lambda_1,i}^k, \mathbf{q}_{\lambda_2,i}^k\}$. Therefore, the updated expressions of the proposed DUAGD are written as

$$\mathbf{f}_i^{k+1} = \mathbf{f}_i^k - \boldsymbol{\mu}_{\mathbf{f},i}^k \circ \nabla_{\mathbf{f}_i^k} L + \mathbf{q}_{\mathbf{f},i}^k, \tag{22}$$

$$\mathbf{\Phi}_i^{k+1} = \mathbf{\Phi}_i^k - \boldsymbol{\mu}_{\mathbf{\Phi},i}^k \circ \nabla_{\mathbf{\Phi}_i^k} L + \mathbf{q}_{\mathbf{\Phi},i}^k, \tag{23}$$

$$\lambda_{1,i}^{k+1} = \lambda_{1,i}^k + \mu_{\lambda_1,i}^k \nabla_{\lambda_{1,i}^k} L + q_{\lambda_1,i}^k, \tag{24}$$

$$\lambda_{2,i}^{k+1} = \lambda_{2,i}^k + \mu_{\lambda_2,i}^k \nabla_{\lambda_{2,i}^k} L + q_{\lambda_2,i}^k, \tag{25}$$

where $\{\boldsymbol{\mu}_{\mathbf{f},i}^k, \boldsymbol{\mu}_{\mathbf{\Phi},i}^k, \mu_{\lambda_1,i}^k, \mu_{\lambda_2,i}^k\}$ and $\{\mathbf{q}_{\mathbf{f},i}^k, \mathbf{q}_{\mathbf{\Phi},i}^k, q_{\lambda_1,i}^k, q_{\lambda_2,i}^k\}$ are trainable parameters, which are used to update the optimization variables $\{\mathbf{f}_i^k, \mathbf{\Phi}_i^k, \lambda_{1,i}^k, \lambda_{2,i}^k\}$ at the k-th layer of the i-th iteration. And $\{\nabla_{\mathbf{f}_i^k} L, \nabla_{\mathbf{\Phi}_i^k} L, \nabla_{\lambda_{1,i}^k} L, \nabla_{\lambda_{2,i}^k} L\}$ are the gradients of the optimization variables in the k-th layer to the loss function L. $\circ$ denote the Hadamard product of two vectors/matrices. Fig. 2 shows the structure of DU neural network based on GD. It can be seen that the structure of the DU algorithm is obtained by unfolding the GD algorithm into a multi-layer structure composed of K successive layers. The channel sample gain matrix input is $\mathcal{H} = \{\mathbf{h}_{tw}, \mathbf{h}_{tb}, \mathbf{h}_{tr}, \mathbf{G}_{ts}, \mathbf{g}_{sw}, \mathbf{g}_{sb}, \mathbf{g}_{sr}\}$. Through the enlarged part in the red dashed rectangle, we can see that each layer of the DU network has same structure. The operations $\boldsymbol{\gamma}_{\mathbf{f}}$, $\boldsymbol{\gamma}_{\mathbf{\Phi}}$, γ_{λ_1} and γ_{λ_2} represent (22), (23), (24) and (25), respectively. For each update, the structure in the black dashed rectangle illustrates how the trainable parameters are used in the GD update process. In the last layer, the beamforming and Lagrange

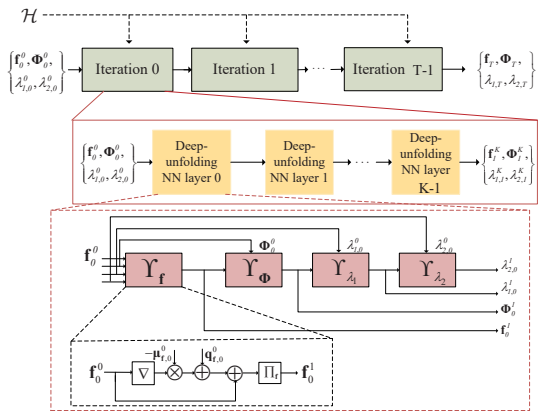

Fig. 2. Deep unfolding algorithm for joint optimization beamforming.

multipliers are conveyed to the loss function which is used to update network parameters by back propagation. Specifically, the trainable parameters are updated with the Adam optimizer by calculating the average gradient of a mini-batch loss function. Such as $\mu^k_{\mathbf{f},i+1} = \mu^k_{\mathbf{f},i} - \alpha^i \cdot \mathrm{Adam}\left(\nabla_{\mu^k_{\mathbf{f},i}} L\right)$, where α^i is the learning rate. The other trainable parameters are updated in the same way. As in the GD algorithm, $\mathbf{f}$, $\mathbf{\Phi}$, λ_1, and λ_2 in each layer are scaled according to (19), (20) and (21) to satisfy the maximum transmission power constraint, unit modulus constraint and the non-negativity constraint, respectively. See **Algorithm** 1 for the specific process of network training.

Algorithm 1 Deep Unfolding algorithm based on GD

Given the samples number J, the layers number K, the maximum number of iterations T, the batch size N_b and learning rates. Initialize trainable parameters and optimization variables $\left\{\mathbf{f}^0_0, \mathbf{\Phi}^0_0, \lambda^0_{1,0}, \lambda^0_{2,0}\right\}$.
for $i = 0 : T$ **do**
  for $j = 0 : N_b$ **do**
    for $k = 0 : K$ **do**
      Calculate the gradient of optimization variables $\left\{\mathbf{f}^k_i, \mathbf{\Phi}^k_i, \lambda^k_{1,i}, \lambda^k_{2,i}\right\}$ and update its by (22)-(25).
      The optimization variables are scaled based on (19)-(21).
    end for
    The loss function is calculated according to (13).
  end for
  Average the loss function of N_b channel samples and calculate the gradient of trainable parameters. Then the trainable parameters are updated by Adam optimizer.
end for
output $\mathbf{f}, \mathbf{\Phi}, \lambda_1, \lambda_2$

C. Computational Complexity

Firstly, we discuss the network parameters dimension of the proposed DUAGD algorithm, which is $2\left(L + M^2 + 1 + 1\right)$ in each layer. As for the OADNN, the computational complexity is $\mathrm{O}\big(\sum_{l=1}^{N_{\mathbf{f}}} F_{\mathbf{f},l} F_{\mathbf{f},l+1} + \sum_{l=1}^{N_{\mathbf{\Phi}}} F_{\mathbf{\Phi},l} F_{\mathbf{\Phi},l+1} + 2\sum_{l=1}^{N_{\lambda}} F_{\lambda,l} F_{\lambda,l+1}\big)$, where $N_{\mathbf{f}}$, $N_{\mathbf{\Phi}}$ and N_{λ} represent the number of layers of the neural network of the active beamforming, the passive beamforming and the Lagrangian multipliers, respectively. And $F_{\mathbf{f},l}$, $F_{\mathbf{\Phi},l}$ and $F_{\lambda,l}$ are the output sizes of these neural networks at the l-layer, respectively. The complexity of GD algorithm in the paper is given by $\mathrm{O}\left(TJS\left(L + M^2\right)\right)$, where T is the number of iterations, J denotes the number of random samples and the size of the testing data is S. The computational complexity of the DUAGD is $\mathrm{O}\left(KJS\left(L + M^2\right)\right)$, where K is the number of layers. Since $K \ll T$, we can see that the complexity of DUAGD proposed in this paper is lower than that of iterative GD algorithm. Moreover, compared with OADNN, the computational complexity of DUAGD is also lower.

IV. Numerical Results

In this section, the performance of DUAGD is verified by numerical results. PTx is considered to be equipped with 4 antennas ($L = 4$). Considering a two-dimensional coordinate system where PTx, PRx, SRx (Bob), RIS (Alice), and Willie are located at $(0, 0)$ m, $(80, 10)$ m, $(90, 10)$ m, $(100, 0)$ m, and $(100, 20)$ m, respectively. The simulation are implemented averages over 1000 independent channel implementations. There are two parts for each channel response, where large-scale fading is related to distance and which is represented as $\chi_{ij} = \beta_0 (\frac{d_{ij}}{d_0})^{-\alpha_{ij}}$, where $ij \in \{tw, ts, tr, tb, sw, sr, sb\}$ represents different channels. d is the distance between nodes i and j. When the reference distance is 1 m, the channel power gain β_0 is set to -30 dB. α_{ij} is the path loss index, where we set $\alpha_{ts} = 2.2$, $\alpha_{tw} = 4.2$, $\alpha_{tb} = 4.2$, $\alpha_{tr} = 4.2$, $\alpha_{sw} = 3$, $\alpha_{sb} = 3$ and $\alpha_{sr} = 3$, respectively. We set the number of layers as $K = 8$, the batch size as $N_b = 20$ and the maximum number of iterations $T = 50$. The remaining system parameters are: $N = 50$, $\sigma_r^2 = -90$ dBm, $\sigma_b^2 = -90$ dBm and $\sigma_w^2 = -90$ dBm [3]. In addition, a small-scale fading component using the Rician fading channel model, which is written as $\mathbf{h} = L_1\big(\sqrt{\frac{\varepsilon}{\varepsilon+1}}\mathbf{h}^{LoS} + \sqrt{\frac{1}{\varepsilon+1}}\mathbf{h}^{NLoS}\big)$, where $\mathbf{h} \in \mathcal{H} = \{\mathbf{h}_{tw}, \mathbf{h}_{tb}, \mathbf{h}_{tr}, \mathbf{G}_{ts}, \mathbf{g}_{sw}, \mathbf{g}_{sb}, \mathbf{g}_{sr}\}$. L_1 denotes the path loss and ε is the Rician factor. $\mathbf{h}^{LoS}$ is the line-of-sight (LoS) component and $\mathbf{h}^{NLoS} \sim \mathcal{CN}(0, 1)$ is the non-line-of-sight (NLoS) component.

To show the performance of the DUAGD, we compare the results with the following schemes. i) Optimization algorithm based on DNN (OADNN): By using DNN to approximate input and output mapping, the optimal beamforming are obtained by training DNN. ii) Random beamforming policy: We randomly select the reflection coefficients of RIS without updating them.

In Fig. 3, we plot the convergence behavior of all algorithms. We fixed the transmission power $P_s = 10$ dBm and the number of reflection units of RIS M = 40. The maximum rate of the DUAGD is higher than that of the OADNN and the random beamforming policy. This shows that RIS passive beamforming optimization is effective. In addition, the number of iterations of DUAGD is less than that of OADNN.

Fig. 4 plots the relationship between the maximum rate and the maximum transmitted power P_s for DUAGD and random beamforming policy in DUAGD. Firstly, we observe that the maximum rate of two schemes increases with P_s. Secondly, the maximum rate of the RIS optimization scheme increases

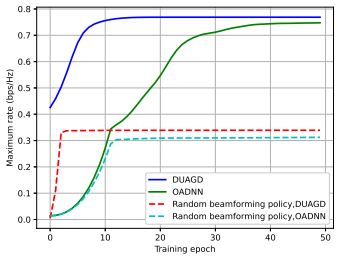

Fig. 3. Convergence behavior of different algorithms.

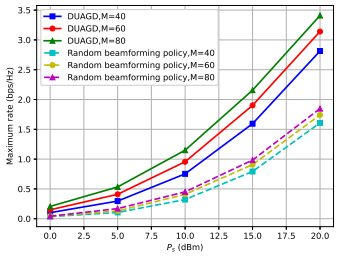

Fig. 4. Maximum rate versus the maximum transmit power of PTx.

significantly with the increase of P_s. And the performance of DUAGD is better than the random beamforming policy scheme. Thus, it is a promising method to deploy RIS to improve the security of wireless communication system. Thirdly, the performance of two schemes increase as M increases. The performance of DUAGD is better than that of random beamforming policy, and their performance gap increases with the increase of M. This is because the designing of joint active and passive beamforming has become more flexible with the more reflected elements.

V. Conclusion

In this paper, we have proposed an RIS-assisted MISO covert SR system, which the eavesdropper Willie detects the passive signals from RIS (Alice) to SRx (Bob). To maximize the achievable rate of PTx, the Lagrangian duality method first was adopted to transform optimization problem with constraint into the dual problem, and the DUAGD have been considered to solve the Lagrangian dual problem. The simulation results showed that the performance of the DUAGD is better compared with that of OADNN and random beamforming policy.

APPENDIX A

In order to make the communication more reliable, we assume that SRx has strong computing power, and adopt the maximum likelihood (ML) detection method to jointly decode $s(l)$ and c in (3). In (3), SRx receives the direct link signal from PTx and the reflected link signal from RIS. When decoding $s(l)$ and c, the signal from RIS is regarded as a multi-path component. Assuming that c can be completely decoded, the covariance matrix of the signal and noise is written by

$$\Gamma_b = |\mathbf{h}_{tb}\mathbf{f} + \mathbf{g}_{sb}\mathbf{\Phi}\mathbf{G}_{ts}\mathbf{f}c|^2. \tag{26}$$

The achievable rate of SRx is expressed as

$$R_b = E_c\left[\log_2\left(1+\Gamma_b\right)\right]. \tag{27}$$

As the N symbol periods of $s(l)$ are covered within the symbol period of c, we can get the SNR of decoded c by using maximum ratio combining, which is expressed as

$$\gamma_b = \frac{\sum_{n=1}^{N}\left|\mathbf{g}_{sb}\mathbf{\Phi}\mathbf{G}_{ts}\mathbf{f}s(n)\right|^2}{\sigma_b^2} \overset{(a)}{\approx} \frac{N\left|\mathbf{g}_{sb}\mathbf{\Phi}\mathbf{G}_{ts}\mathbf{f}s(n)\right|^2}{\sigma_b^2}, \tag{28}$$

where (a) holds, because if $N \gg 1$, the arithmetic mean and the statistical expected value are approximately equal.

References

[1] C. Wang, Z. Li, J. Shi, and D. W. K. Ng, "Intelligent reflecting surface-assisted multi-antenna covert communications: Joint active and passive beamforming optimization," *IEEE Trans. Commun.*, vol. 69, no. 6, pp. 3984–4000, 2021.

[2] C. Chen, M. Wang, B. Xia, Y. Guo, and J. Wang, "Performance Analysis and Optimization of IRS-aided Covert Communication with Hardware Impairments," *IEEE Trans. Veh. Technol.*, 2022.

[3] X. Zhou, S. Yan, Q. Wu, F. Shu, and D. W. K. Ng, "Intelligent reflecting surface (IRS)-aided covert wireless communications with delay constraint," *IEEE Trans. Wireless Commun.*, vol. 21, no. 1, pp. 532–547, 2021.

[4] Y.-C. Liang, Q. Zhang, E. G. Larsson, and G. Y. Li, "Symbiotic radio: Cognitive backscattering communications for future wireless networks," *IEEE Trans. on Cogn. Commun. Netw.*, vol. 6, no. 4, pp. 1242–1255, 2020.

[5] X. Chen, J. An, Z. Xiong, C. Xing, N. Zhao, F. R. Yu, and A. Nallanathan, "Covert communications: A comprehensive survey," *IEEE Commun. Surveys Tuts.*, 2023.

[6] Z. Wang, M. Wang, B. Xia, Y. Guo, and J. Wang, "IRS-aided covert communications over correlated fading channels: Analysis and optimization," *IEEE Wireless Commun. Lett.*, 2023.

[7] H. Song, M. Zhang, J. Gao, and C. Zhong, "Unsupervised learning-based joint active and passive beamforming design for reconfigurable intelligent surfaces aided wireless networks," *IEEE Commun. Lett.*, vol. 25, no. 3, pp. 892–896, 2020.

[8] J. Gao, C. Zhong, X. Chen, H. Lin, and Z. Zhang, "Unsupervised learning for passive beamforming," *IEEE Commun. Lett.*, vol. 24, no. 5, pp. 1052–1056, 2020.

[9] M. Zhu, T.-H. Chang, and M. Hong, "Learning to beamform in heterogeneous massive MIMO networks," *IEEE Trans. Wireless Commun.*, 2022.

[10] L. Pellaco, M. Bengtsson, and J. Jaldén, "Deep unfolding of the weighted MMSE beamforming algorithm," *arXiv preprint arXiv:2006.08448*, 2020.

[11] S. Shi, Y. Cai, Q. Hu, B. Champagne, and L. Hanzo, "Deep-unfolding neural-network aided hybrid beamforming based on symbol-error probability minimization," *IEEE Trans. Veh. Technol.*, 2022.

[12] Y. Cao, T. Lv, and W. Ni, "Two-timescale optimization for intelligent reflecting surface-assisted MIMO transmission in fast-changing channels," *IEEE Trans. Wireless Commun.*, vol. 21, no. 12, pp. 10424–10437, 2022.

[13] R. Long, Y.-C. Liang, H. Guo, G. Yang, and R. Zhang, "Symbiotic radio: A new communication paradigm for passive Internet of Things," *IEEE Internet Things J.*, vol. 7, no. 2, pp. 1350–1363, 2019.

[14] D. Tse and P. Viswanath, *Fundamentals of Wireless Communication*. Cambridge university press, 2005.

[15] B. A. Bash, D. Goeckel, and D. Towsley, "Limits of reliable communication with low probability of detection on AWGN channels," *IEEE J. Sel. Areas Commun.*, vol. 31, no. 9, pp. 1921–1930, 2013.

[16] S. Yan, B. He, X. Zhou, Y. Cong, and A. L. Swindlehurst, "Delay-intolerant covert communications with either fixed or random transmit power," *IEEE Trans. Inf. Forensics Security.*, vol. 14, no. 1, pp. 129–140, 2018.

[17] A. Shapiro, D. Dentcheva, and A. Ruszczynski, *Lectures on stochastic programming: modeling and theory*. SIAM, 2021.

[18] A. Hakobyan, G. C. Kim, and I. Yang, "Risk-aware motion planning and control using CVaR-constrained optimization," *IEEE Robot. Autom. Lett.*, vol. 4, no. 4, pp. 3924–3931, 2019.